Urban Ecosystems, 8: 349–361, 2005

Tree health mapping with multispectral remote sensing data at UC Davis, California

QINGFU XIAO* qxiao@ucdavis.edu
Department of Land, Air, and Water Resources, University of California, Davis

E. GREGORY McPHERSON
Center for Urban Forest Research, Pacific Southwest Research Station, USDA Forest Service

Abstract. Tree health is a critical parameter for evaluating urban ecosystem health and sustainability. Traditionally, this parameter has been derived from field surveys. We used multispectral remote sensing data and GIS techniques to determine tree health at the University of California, Davis. The study area (363 ha) contained 8,962 trees of 215 species. Tree health conditions were mapped for each physiognomic type at two scales: pixel and whole tree. At the pixel scale, each tree pixel within the tree crown was classified as either healthy or unhealthy based on vegetation index values. At the whole tree scale, raster based statistical analysis was used to calculate tree health index which is the ratio of healthy pixels to entire tree pixels within the tree crown. The tree was classified as healthy if the index was greater than 70%. Accuracy was checked against a random sample of 1,186 trees. At the whole tree level, 86% of campus trees were classified as healthy with 88% mapping accuracy. At the pixel level, 86% of the campus tree cover was classified as healthy. This tree health evaluation approach allows managers to identify the location of unhealthy trees for further diagnosis and treatment. It can be used to track the spread of disease and monitor seasonal or annual changes in tree health. Also, it provides tree health information that is fundamental to modeling and analysis of the environmental, social, and economic services produced by urban forests.

Keywords: Urban forestry, tree health index, tree health mapping, remote sensing data

Introduction

Urban forests are a significant natural resource that affects the majority of the population, most of whom live in cities. Trees in urban forests not only provide aesthetic and recreational benefits, they also reduce air pollution and storm runoff, conserve energy, store carbon, provide protection from ultraviolet radiation, create habitat for wildlife, and moderate air temperatures. All of these benefits are influenced by tree health. Tree health directly affects the urban ecosystem's function and performance (Xiao and McPherson, 2002). Monitoring urban forest tree health has traditionally relied on ground surveys and monitoring programs (Cumming *et al.*, 2001; Alexander and Palmer, 1999). These methods are costly and require considerable human resources.

*Author to whom all correspondence should be address. Qingfu Xiao, CUFR, c/o Department of Plant Sciences, Mail Stop 6, University of California, One Shields Avenue, Davis, CA 95616-8780, Tel.: +530-752-6804; Fax: +530-752-6634

Remote sensing data has been widely used in land use, land cover, and vegetation mapping for urban and rural forests (Erikson, 2004; Xiao *et al.*, 2004; Pouliot *et al.*, 2002; Ustin and Xiao, 2001). In rural forests, application of remotely sensed data has been expanded to forest health monitoring (Diem, 2002; Olthof and King, 2000). Xiao *et al.* (2004) demonstrated the potential of urban forest tree species mapping by using high resolution spectral remote sensing data and multiple masking techniques. The use of multiple-masking techniques shifts the focus to the target land cover types only, thus reducing confounding noise during spectral analysis. Vegetation indices, such as Normalized difference vegetation index (NDVI), have been widely used for greenness or health condition detection (Maselli, 2004; Birky, 2001; Richardson and Everitt, 1992). High spatial resolution remotely sensed color infrared data have been widely used by local government planning and natural resources agencies. These data are typically acquired from three spectrum windows: near infrared (NIR), red, and green.

Mapping tree health in an urban setting is difficult because most trees are on private property and difficult to access in the field. Although remote sensing can rectify this problem, it is more difficult to distinguish individual tree species from imagery than from the ground. Cities contain of the wide variety of tree species and their distribution is often fragmented. Although the spectral information is limited with color infrared data, it contains the red and NIR bands that are critical for urban vegetation mapping. By using this type of remote sensing data with a 20 cm resolution, it is possible to acquire a rich set of information on the canopy at and below the individual tree scale.

Objectives

The objectives of this investigation are twofold: Development of an urban forest tree-health mapping method based on remotely sensed multispectral data and GIS data layers, and use of this method to map urban forest tree health.

Methods

Study site

The study site is the campus core area of the University of California, Davis (121°46′32″ W, 38°32′09″ N). The campus core area covers 3.6 km^2 (897.0 acre) and is located in the heart of the Central Valley, between the Coast Range to the west and the Sierra Nevada to the east. The topography is relatively flat. The campus is surrounded by agricultural land and residential neighborhoods. Campus development started in the early 1900's as a State Agriculture School. At that time, the land cover types were farm land, dirt roads, and trees. After a century of development, the primary land cover types are buildings, parking lots, streets, roads and paths, and trees and grass (figure 1). Larger trees are in the older sections of the campus. The climate is Mediterranean, summers are sunny, hot, and dry while winters are wet but not cold, it rarely snows. On average, 90% of the average annual precipitation (446 mm) occurs between November and April. Irrigation is the only water resource for plants during the summer.

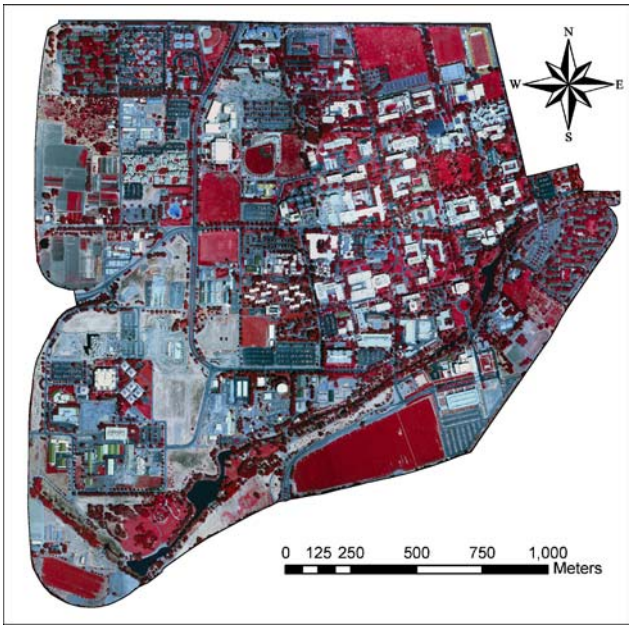

Figure 1. Study site.

Data set

High resolution multispectral remote sensing data, GIS base layers, and field tree samples were acquired for this investigation during the summers of 2003 and 2004. Color infrared imagery for the entire campus was collected on August 8, 2003 by WAC Corporation, Inc. Eugene, Oregon (Camera type: Wild RC10. Lens type: Wild Normal Aviotar/4. Nominal focal length: 305 mm). This dataset included three spectral bands (near infrared (NIR), red, and green at 1 to 4,800 spatial resolution. These frame images were scanned at 600DPI and mosaicked using ERDAS IMAGINE OrthoBASE (ERDAS, Inc. 2002). The mosaicked image was geo-referenced to the GIS base layers. The analyses were performed using ArcGIS software (Environmental Systems Research Institute, Inc. 2004). The GIS layers included buildings, parking lots, roads, and paths. Also, a tree inventory layer was created based on the campus tree survey that was updated in the summer 2003 by Great Scott Tree Service, Inc. Stanton, California. The tree survey included tree location, species, and dimensions (e.g., tree trunk diameter at breast height (dbh), height, and crown diameter). Trees in the Arboretum and Environmental Horticulture research field were excluded from this inventory because they were managed differently than the rest of the campus trees. The inventory contained 8,962 trees comprising 215 species. Forty species accounted for 80% of the population. Trees were further classified by their physiognomic type (broadleaf deciduous, broadleaf evergreen, conifer, and palm) and mature size (tree height less than 10 m for small, 10–20 m for medium, $>$ 20 m for large) (Table 1). These 8,962 trees covered 0.46 km^2 (115 ac). Broadleaf deciduous

Table 1. The campus tree composition by species, tree number, and canopy cover. Data were from the existing campus tree inventory. A total of 8,962 trees covered 0.46 km^2 (115 ac). Broadleaf deciduous trees were the most abundant tree type (55%). More than half (59%) of the trees on campus were large trees and they accounted for 74% of the canopy cover.

Type[a]	Number of species	Number of trees	Number ot trees (%)	Canopy cover (%)
BDL	41	2,421	27.0	38.3
BDM	34	1,422	15.9	14.3
BDS	32	1,075	12.0	4.8
Total	107	4,918	54.9	57.4
BEL	19	956	10.7	19.5
BEM	16	499	5.6	3.8
BES	26	361	4.0	2.8
Total	61	1,816	20.3	26.1
CEL	30	1,910	21.3	16.0
CEM	7	240	2.7	0.2
CES	3	15	0.2	0.1
Total	40	2,165	24.2	16.3
PEL	2	10	0.1	0.1
PEM	3	17	0.2	0.0
PES	2	36	0.4	0.1
Total	7	63	0.7	0.1
Grand total	215	8,962	100.0	100.0

[a]BD = Broadleaf Deciduous; BE = Broadleaf Evergreen; CE = Conifer; PE = Palm; L = Large; M = Medium; S = Small.

trees were the most abundant tree type (55%). More than half (59%) of the trees on campus were large trees and they accounted for 74% of the canopy cover. Most of the street trees were not irrigated. They rely on water from their supporting soil or adjacent lawn irrigation.

In summer 2004, two sets of field data were collected. The first set included 81 open growing trees from the existing GIS layer. These were randomly selected from each of the four tree types. Their health was evaluated in the field to develop a health index for each tree type. The tree health index is defined as the ratio of healthy pixels to the entire tree pixels within the tree crown. This data set included 16 unhealthy and 65 healthy trees. The second data set included 1,186 trees randomly selected from the inventory to check the accuracy of the tree health mapping. This data set included 100 species (Table 2).

Vegetation mapping

Vegetation mapping included mapping vegetation cover and tree health. In this study, three types of vegetation were classified: tree, shrub, and grass. Tree health was classified as either healthy or unhealthy. Non-vegetation land covers were not mapped in this study.

The spectral reflectance of vegetation is completely different than the reflectance properties of the`background material' (i.e., water, soil, and pavement). Vegetation absorbs light

Table 2. The number of species and tree types that comprised the random sample used to assess accuracy of the health classification

Type	Number of species	Number of trees
BDL	20	432
BDM	16	170
BDS	15	142
Total	51	744
BEL	11	159
BEM	4	52
BES	8	43
Total	23	254
CEL	19	170
CEM	2	8
CES	1	1
Total	22	179
PEL	1	1
PEM	1	1
PES	2	7
Total	4	9
Grand total	100	1,186

for photosynthesis. In the NIR region, vegetation has a high reflectance, with a very rapid transition to low levels between red and NIR regions at ∼750 nm. This unique character of the vegetation spectrum makes it possible to separate vegetation from background material with remotely sensed multispectral data that at least includes NIR and red region reflectance.

Vegetation indices (VIs) are commonly used to evaluate vegetation based on the vegetations' spectral characteristics in the NIR and red spectral region or at the red edge. A high VI value indicates healthy vegetation and a low value indicates senescent, diseased, foliage damaged, water stressed vegetation, or non-vegetated area. NDVI is a good index for distinguishing vegetation and non-vegetation cover. NDVI is the ratio of the reflectance difference between NIR and red and the sum of the reflectance at NIR and red. Healthy vegetation has a higher NDVI value than unhealthy vegetation.

Tree crown delineation

NDVI was generated from the NIR and red bands for the study area. The NDVI threshold of 20 was used to separate vegetation and non-vegetation (we assumed that each pixel was either vegetation or non-vegetation). The vegetation cover included trees, shrubs, and grass. Tree crowns in parking lots were automatically delineated based on their NDVI values. Non-vegetation pixels inside the tree drip line were excluded to increase accuracy of the analysis results (Meyer *et al.*, 1996; Gougeon, 1995; Leckie *et al.*, 1992).

Trees and shrubs located in parks and along some road sites had the same NDVI values as the surrounding turf grass. Due to the limited spectral information in this remote sensing dataset, we were unable to further separate trees and shrubs from grass based on their spectral characteristics. Rather, we digitized the trees and shrubs based on manual interpretation of the remote sensing imagery.

The tree layer derived from the remotely sensed data was linked to the existing GIS data to obtain the tree information based on the ground survey. The most important information from the existing GIS data layer was the scientific name and dbh class. These data were used to classify trees into different physiognomic types and mature sizes.

Tree health mapping

For the same tree species, a higher NDVI value indicates a healthier tree. Clearly, the leaf size, leaf water content, leaf pigmentation, and the stem structure and non-vegetation background visible in the overhead view strongly affect these indices. NDVI works well in places where vegetation species are homogeneous. In urban forests, where vegetation species are heterogeneous and have diverse backgrounds, tree-health mapping becomes more complex. For example, a healthy, well-grown conifer tree may have the same NDVI value as an unhealthy broadleaf deciduous tree has. To solve this mixing problem, a multiple masking technique (Xiao *et al.*, 2004) was used to perform the tree health mapping for each physiognomic tree type. The first mask was created based on the classification of land cover types. This mask was used to mask out all non-vegetation. The remaining vegetation was mapped into five layers based on the physiognomic tree type. These five layers were broadleaf deciduous, broadleaf evergreen, conifer, palm, and mixed. The mixed layer included shrub and clustered trees. The clustered trees were defined as multiple trees that had overlapping crowns.

Tree health was first evaluated at the pixel scale. A pixel-based analysis of the NDVI value and tree health from the field survey was performed for each tree type. For each tree type, the thresholds for both NDVI and health index were determined based on histogram analysis for both healthy and unhealthy trees in the 81-tree sample. The pixels for each tree crown were classified as healthy or unhealthy. The NDVI threshold was 31 for a broadleaf deciduous tree, 30 for a broadleaf evergreen tree, and 24 for both conifer and palm trees. NDVI values above the threshold were classified as healthy pixels, while other values were classified as an unhealthy pixel. The number of healthy pixels, unhealthy pixels, and average NDVI were derived for each tree. Figure 2 shows the field tree health evaluation, average NDVI, and percentage of healthy pixels for all of the broadleaf deciduous trees, 38 of 81 trees that were used to derive the health threshold value. Average NDVI values for all eight unhealthy trees were less than 30 and the percentage of healthy pixels was less than 70.

At the single tree scale, the tree was mapped as either a healthy or unhealthy tree. Healthy pixels, unhealthy pixels, and average NDVI were calculated for each tree based on tree species and all NDVI values under the tree crown. A tree was mapped unhealthy if 30% or more of the pixels were unhealthy and the average NDVI value was less than the threshold for healthy as described in the pixel-based mapping for each tree type.

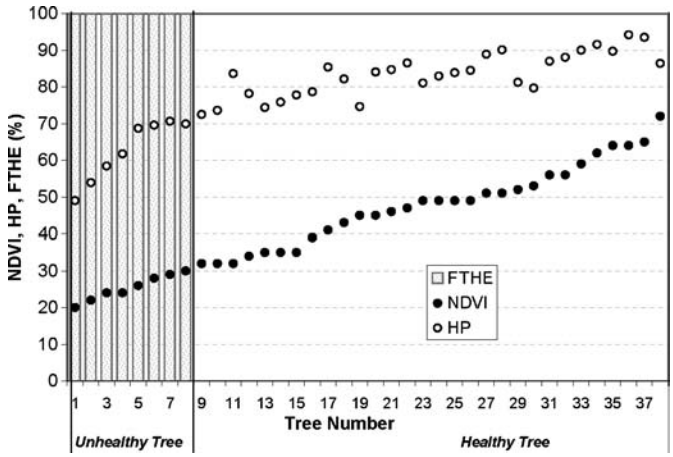

Figure 2. Average NDVI, percentage healthy pixel (HP), and field tree evaluation of the 38 broadleaf deciduous trees. These are all of this tree type in the 81 filed tree samples that were used for develop tree health index. Eight trees were unhealthy from the field tree health evaluation (FTHE). Tree was evaluated as either health (= 0) or unhealthy (= 1). These unhealthy trees had NDVI less than 30 and HP less than 70.

There were 540 mixed trees (9%) excluded from the final analysis at the whole-tree level because they lacked species information or their crowns overlapped. These trees were treated as mixed conifers and evergreens (50%–50%) in the pixel level analysis based on field observations of clustered trees.

Mapping and health classification accuracy assessment

Tree health was presented at two different spatial scales. The raster-based map presented information at the pixel level, which included tree health and vegetation indexes for each pixel of the tree crown. The vector-based map presented information at the whole tree level. Each tree was classified as either healthy or unhealthy. In addition to the initial tree information, the health index, number of healthy pixels, unhealthy pixels, and averaged vegetation index were added to the tree GIS layer for each tree.

The accuracy check for tree health classification was performed at the individual tree level. The confusion matrix (Kohavi and Provost, 1998) was used as the basis for comparison. The study area was uniformly divided into 400 grids. Fifty-six grids were randomly selected for the tree health classification accuracy assessment. All of the 1,186 trees (101 tree species) within these selected grids were surveyed during the summer of 2004 for the health assessment. Each tree was rated as healthy or unhealthy based on protocols described in the Council of Tree and Landscape Appraiser's Guide for Plant Appraisal (Gooding *et al.*, 2000). This protocol requires rating five factors: roots, trunk, scaffold branches, smaller branches and twigs, and foliage. It provides guidelines for assigning five rating points to each factor (extreme problem = 0 or 1, major problem = 2, minor problem = 3, no apparent problem = 4, no problem = 5). Tree health was evaluated based on the total points each

tree received. According to the protocol, trees receiving 19–22 points are classified as in Good condition, while those with 23–25 points are in Excellent condition. Therefore, trees that we surveyed in field that received 19 or more points were classified as healthy, while unhealthy trees received less than 19 points.

Among the five factors used in the field tree health evaluation, remote sensing data are most sensitive for detecting change in foliage health. Information on the other factors was limited by view angle (such as for roots and trunks) and spatial resolution (such as for small branches and twigs). However, most diseases or abiotic stresses to the roots or bole are ultimately expressed as changes in the density, chemistry, color, and moisture content of the foliage.

Results and discussion

Vegetation cover

The vegetation coverage of the campus core area was 37% (135.3 ha). Of this amount, 53% (71.4 ha) was cover by tree /shrub and 47% (63.9 ha) was covered by grass. The campus tree survey conducted during 2004 contained 9,862 individual trees within the core area. Based on the tree inventory, the majority (55%) of campus trees were deciduous trees, accounting for 57% of the total canopy cover. Broadleaf evergreen trees accounted for 20% of the total tree population and 26% of canopy cover, while conifers accounted for 24% of the total tree population and 16% of canopy cover. Palm trees accounted for less than 1% of the total tree population and canopy cover.

Most of the trees were near buildings and along streets and pathways. The spatial distribution of both number of trees and the size of trees were closely related to campus development. Large and old trees were common in the older parts of campus. In the newly developed areas, trees were young, and canopy cover in these areas was relatively low.

Health index

Tree health was mapped as either healthy or unhealthy at both the pixel and single tree levels (Table 3). Broadleaf deciduous and coniferous trees had the highest percentage of unhealthy pixels, 16% and 15%, respectively. Parking lots and streets trees were dominated by deciduous species. In August, when the imagery was acquired, many of these trees were in water stress, which caused a decrease in their photosynthetic activity. For some trees, leaves had begun to fall. Thus, these trees had a lower NDVI value compared to the same species planted in well irrigated areas. Most conifer trees in the study area were large trees. Many were located where they did not receive regular irrigation, thus these trees were in water stress during later summer. Low photosynthetic activities in these trees resulted in a lower NDVI compared to the well irrigated trees. The spatial distribution of tree health is presented in (figure 3) at the pixel scale (figure 3c) and whole tree scale (figure 3d). There were unhealthy trees due primarily to adverse impacts of construction work in both the north and west side of the lot. We selected this parking lot, which had the worst tree health

Table 3. Tree health at the pixel and whole tree level by tree type

	Pixel level					Whole tree level				
	Pixels			%		Trees[b]			%	
Type	H[a]	UNH[a]	Total	H	UNH	H	UNH	Total	H	UNH
BDL	1,196,861	239,905	1,436,766	83.3	16.7	1,494	323	1,817	82.2	17.8
BDM	465,909	74,327	540,236	86.2	13.8	939	131	1,070	87.8	12.2
BDS	153,975	31,619	185,594	83.0	17.0	574	107	681	84.2	15.8
Total	1,816,745	345,851	2,162,596	84.0	16.0	3,007	561	3,568	84.3	15.7
BEL	643,191	73,709	716,900	89.7	10.3	551	72	623	88.4	11.6
BEM	132,362	15,232	147,594	89.7	10.3	258	37	295	87.4	12.6
BES	96,852	9,782	106,634	90.8	9.2	183	26	209	87.7	12.3
Total	872,405	98,723	971,128	89.8	10.2	992	135	1,127	88.0	12.0
CEL	512,734	92,656	605,390	84.7	15.3	890	132	1,022	87.1	12.9
CEM	7,557	1,310	8,867	85.2	14.8	38	8	46	83.2	16.8
CES	1,682	353	2,035	82.7	17.3	4	1	6	78.9	21.1
Total	521,973	94,319	616,292	84.7	15.3	932	141	1,073	86.9	13.1
PEL	3,895	183	4,078	95.5	4.5	9	0	9	100.0	0.0
PEM	1,113	40	1,153	96.5	3.5	4	4	8	50.0	50.0
PES	4,314	466	4,780	90.3	9.7	26	0	26	100.0	0.0
Total	9,322	689	10,011	93.1	6.9	39	4	43	90.7	9.3
Grand Total	3,220,445	539,582	3,760,027	85.6	14.4	4,970	841	5,811	85.5	14.5

[a]H = Healthy UNH = Unhealthy.
[b]540 trees were excluded in this table because they were not single trees in the GIS data set.

among all parking lots on campus, to show how tree mapping was presented at the pixel and whole tree scales.

In the study area, 86% of the trees were healthy (Table 3). Palms had the highest percentage of healthy trees (91%), followed by broadleaf evergreen (88%), conifer (87%), and deciduous (84%). These results compared well with results at the pixel scale.

By mapping tree health at these two different spatial scales, urban foresters can obtain critical information for tree management. For example, at the individual tree level data can be compiled to reflect the overall health of the tree population. At the pixel level it is possible to identify the relative magnitude of stress within individual tree crowns, and use this information to prioritize inspections to diagnose and treat health threats.

Health classification accuracy

Tree health classification accuracy was checked at the single tree level with 1,186 trees. Field survey assessments agreed with remotely sensed classification for 88% of the sample.

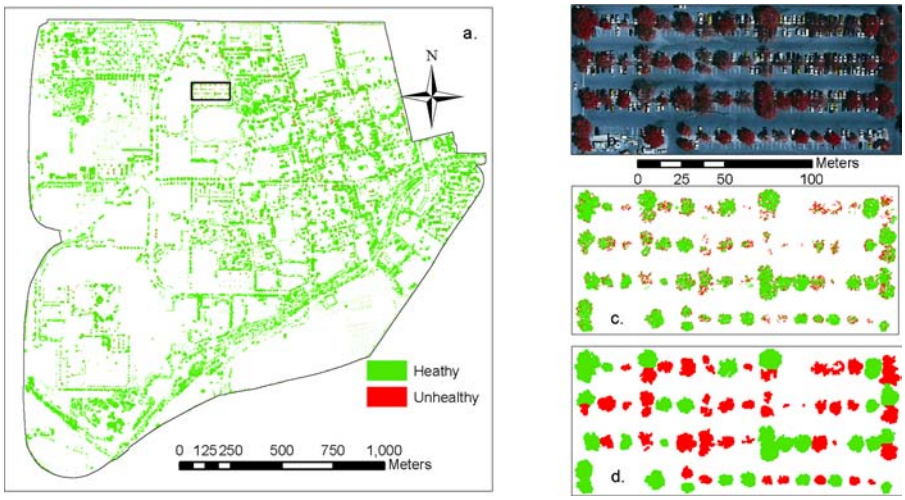

Figure 3. Spatial distribution of tree health. A parking lot is expanded for viewing in (Figure 3(a)). Figure 3(b) shows the color infrared image. Figure 3(c) shows tree health at the pixel scale, and figure 3(d) shows tree health at the whole tree scale. There were unhealthy trees due primarily to adverse impacts of construction work in both the north and west side of the lot.

The accuracy for deciduous trees was 86% but varied with tree size. Accuracies were 80%, 94%, and 94% for large, medium, and small deciduous trees, respectively. Classification accuracies were 92%, 91%, and 89% for broadleaf evergreen, conifer, and palm trees, respectively (Table 4). Small conifer and all of the palm species accounted for less than 0.5% of the total tree population. The accuracy values for these trees carried less weight than values for more abundant tree types in the classification of overall health.

Both tree crown structure and the view angle of the remote sensing data collection system affect mapping accuracy. Differences in crown structure lead to variations in within crown shadows. These variations could result in underestimates of NDVI value of tree pixels under the shadow, and thus underestimate the number of healthy pixels. Overlapping of tree and turf grass could lead to underestimating of turf grass coverage and unhealthy trees due to remote sensing data acquired from nadir (overhead view) angle. The remotely sensed data detected tree health from above the tree crown. Thus, if the top of the crown had a healthy leaf layer, the tree was classified as a healthy tree regardless of conditions lower in the crown. Dead branches in the tree crown were the main cause for misclassification, especially for the large deciduous trees. Tree health derived from remotely sensed data is more sensitive to water stress, disease, and insect attacks that directly affect the leaves than to poor tree health caused by senescence within the crown (Jackson *et al.*, 1981). The remotely sensed data were sensitive to the health of the tree's foliage, which may or may not be directly related to problems with the roots or bole. As a tree becomes increasingly unhealthy and the amount of foliage decreases, this remote sensing detection system may register increasing error. Dead trees, with a low NDVI value, may not be detected without a GIS tree database. On the other hand, water stress can change the infrared signal, but

Table 4. Tree health classification accuracy by tree physiognomic type. Columns show the number of trees classified as healthy (H) and unhealthy (UH) based on field tree evaluation and the rows show remote sensing classification (Classified). The last columns show the number and percentage of trees that were correctly classified. Overall, 88% were correctly classified

	LH	LU	MH	MU	SH	SU	Total	Accuracy
Broadleaf deciduous								
LH[a]	277	41					318	
LU	45	69					114	80.1%
MH			145	9			154	
MU			1	15			16	94.1%
SH					127	6	133	
SU					3	6	9	93.7%
Total	322	110	146	24	130	12	744	85.9%
Broadleaf evergreen								
LH	143	6					149	
LU	4	6					10	93.7%
MH			44	2			46	
MU			4	2			6	88.5%
SH					39	4	43	
SU					0	0	0	90.7%
Total	147	12	48	4	39	4	254	92.1%
Conifer								
LH	148	9					157	
LU	5	8					13	91.8%
MH			6	2			8	
MU			0	0			0	75.0%
SH					1	0	1	
SU					0	0	0	100.0%
Total	153	17	6	2	1	0	179	91.1%
Palm								
LH	1	0					1	
LU	0	0					0	100.0%
MH			1	0			1	
MU			0	0			0	100.0%
SH					6	1	7	
SU					0	0	0	85.7%
Total	1	0	1	0	6	1	9	88.9%

(a L = larger, M = Medium, S = Small, H = Healthy, U = Unhealthy.)

not necessarily be detected by field crews assessing tree health. This could lead to remote sensing detecting unhealthy trees, but the field assessment evaluating the tree as healthy. As such, this technique provides only one of the indications of health.

We did not further investigate nor quantify mapping errors caused by view angle and crown structural variation in this study. However, these errors should be small. Most trees in this urban setting were isolated, thus the nadir view angle minimized the shadow effect caused by tree crown structure and adjacent trees.

We did not examine the cost-effectiveness of remote sensing to detect tree health versus ground-based assessments. Field surveys can provide detailed information on a variety of tree health indicators, and identify the priority of different management needs. This remote sensing approach might be best applied in large scale assessments, allowing the manager to target more intensive work where tree health is most compromised. Also, it might be used as a form of detection monitoring to regularly assess the effectiveness of measures used to improve tree health.

Conclusions

Urban tree health was assessed using multispectral high spatial resolution remotely sensed data. This urban tree mapping method may be best applied for large scale assessments, where it can provide valuable information to urban foresters for management. Tree health mapping at the single tree level could be used to identify the need for tree removal and replacement. Patterns at the pixel level could provide information for determining the need for pruning, irrigation, or pest/disease treatment. This tree health evaluation approach allows managers to identify the location of unhealthy trees for further diagnosis and treatment. It can be used to track the spread of disease and monitor seasonal or annual changes in tree health. In conjunction with a tree inventory, data from this analysis can be used to budget costs for treatment and removal of trees. Also, it provides tree health information that is fundamental to modeling and analysis of the environmental, social, and economic services produced by urban forests.

Acknowledgments

We wish to acknowledge Scott Maco and Chad Delany (Center for Urban Forest Research, USDA Forest Service) for their assistance in the field sampling and comments on improving this manuscript. This research was supported in part by funds provided by the University of California Davis and by the Pacific Southwest Research Station, Forest Service, U.S. Department of Agriculture.

References

Alexander, S.A. and Palmer, C.J. (1999) Forest health monitoring in the United States: First four years. *Environ. monit. assess.* **55**, 267–277.

Birky, Alicia K. (2001) NDVI and a simple model of deciduous forest seasonal dynamics. *Ecol. Model.* **143**, 43–58.

Cumming, A.B., Galvin, M.F., Rabaglia, M.F.R.J., Cumming, J.R., Twardus, D.B. (2001) Forest health monitoring protocol applied to roadside trees in Maryland. *J. Arboric.* **27**, 126–138.

Diem, J.E. (2002) Remote Assessment of Forest Health in Southern Arizona, USA: Evidence for Ozone-Induced Foliar Injury. *Environ.l Manage.* **29**, 373–384.

Erikson, M. (2004) Species classification of individually segmented tree crowns in high-resolution aerial images using radiometric and morphologic image measures. *Remote Sens. Environ.* **91**, 469–477.

Gooding, R.F., Ingram, J.B., Urban, J.R., Bloch, L.B. and Steigerwaldt, W.M., Harris, R.W., Allen, E.N. (2000) *Guide for Plant Appraisal*, 9th Ed. International Society of Arboriculture. pp. 143.

Gougeon F. A. (1995) Comparison of possible multispectral classification schemes for tree crowns individually delineated on high spatial resolution MEIS images. *Can. J. Remote Sens.* **21**, 1–9.

Jackson, R.D., Idso, S.B., Reginato, R.J. and Pinter, P.J. Jr. (1981) Crop temperature as a crop water stress indicator. *Water Resour. Res.* **17**, 1133–1138.

Kohavi, R. and Provost, F. (1998) Glossary of Terms. *Mach. Learn.* **30**, 271–274.

Leckie, D.G, Yuan, X., Ostaff, D.P., Piene, H. and Maclean, D.A. (1992) Analysis of high resolution multispectral MEIS imagery for spruce budworm damage assessment on a single tree basis. *Remote Sens. Environ.* **40**, 125–136.

Maselli, Fabio (2004). Monitoring forest conditions in a protected Mediterranean coastal area by the analysis of multiyear NDVI data. *Remote Sens. Environ.* **89**, 423–433.

Meyer, P., Staenz, K. and Itten, K.I. (1996) Semi-automated procedures for tree species identification in high spatial resolution data from digitized colour infrared-aerial photography. *ISPRS J. Photogramm Remote Sens.* **51**, 5–16.

Olthof, I. and King, D.J. (2000) Development of a Forest Health Index Using Multispectral Airborne Digital Camera Imagery. *Can. J. Remote Sens.* **26**, 166–176.

Pouliot, D.A., King, D.J., Bell, F.W. and Pitt, D.G. (2002) Automated tree crown detection and delineation in high-resolution digital camera imagery of coniferous forest regeneration. *Remote Sens. Environ.* **82**, 322–334.

Richardson, A.J. and Everitt, J.H. (1992) Using Spectral Vegetation Indices to Estimate Rangeland Productivity. *Geocarto Int.* **1**, 61–69.

Ustin, S.L. and Xiao, Q.F. (2001) Mapping successional boreal forests in interior central Alaska. *Int. J. Remote Sens.* **22**, 1779–1797.

Xiao, Q.F., Ustin, S.L. and McPherson, E.G. (2004) Using AVIRIS data and multiple-masking techniques to map urban forest tree species. *Int. J. Remote Sens.* **25**, 5637–5654.

Xiao, Q.F. and McPherson, E.G. (2002) Rainfall interception of Santa Monica's municipal urban forest. *Urb. Ecosyst.* **6**, 291–302.